Nuclear Instruments and Methods 211 (1983) 343–351
North-Holland Publishing Company

ON THE MEASUREMENT OF THE MOMENTUM OF 19 GeV/c ELECTRONS IN A HEAVY LIQUID BUBBLE CHAMBER

G. HARIGEL
CERN, Geneva, Switzerland and Columbia University Nevis Laboratories, Irvington, NY 10533, USA

C. BALTAY and M. HIBBS
Columbia University Nevis Laboratories, Irvington, NY 10533, USA

Received 27 October 1982

The Fermilab 15-ft bubble chamber was exposed to an electron beam of 19 GeV/c momentum. The chamber was filled with a heavy neon–hydrogen mixture (64% atomic Ne, 36% atomic H) and operated with a magnetic field of 3 T. The momentum of the electrons was determined from the bubble chamber pictures using two methods: (a) the measurement of the curvature of the electrons and their shower products, and (b) the measurement of the total track length of the electron and its shower. The momentum, as determined from curvature measurement of the primary electron and the e^+e^- pairs from the radiated gammas was 19.1 ± 7.6 GeV/c.

1. Introduction

The knowledge of the electron momentum is of interest in many experiments, both in hadron and neutrino exposures of heavy liquid bubble chambers. The aim of the present study is to determine the momentum of fast electrons from information contained in the bubble chamber picture, when the electromagnetic shower is (essentially) contained inside the chamber, to compare various methods to achieve this goal, and to estimate their errors. The proposed procedures are suited for non-automatic measuring machines with off-line geometry, such as the tables used at Columbia's Nevis Laboratories.

During a calibration run in an "enriched" electron beam of the Fermilab 15-ft bubble chamber when filled with a heavy neon–hydrogen mixture (64% atomic Ne, 36% atomic H, density 0.76 g/cm^3), 1400 three-view pictures were taken. During the exposure, the beam was tuned to give on the average one 19 GeV/c electron per pulse. There was a contamination of this electron beam by about three to four times as many π^-, which were used to determine the momentum and angles of the incident beam.

2. Possible methods of momentum measurement

Three methods should allow the determination of the momentum of electrons from bubble chamber pictures.

2.1. Method (a)

Measurement of the momenta of the primary electron track and the e^+e^- pairs from radiate gammas from curvature, with correction for energy lost to soft bremsstrahlung [1]. This method does not require that the electromagnetic shower is completely contained within the bubble chamber. It is generally used in experiments with heavy liquid bubble chambers, but its precision has not yet been determined for electrons in the GeV/c momentum range.

Many versions of this method exist, which try in one way or another to take into account multiple scattering and soft and hard bremsstrahlung losses. Here, we limit ourselves to a short description of TVGP *. The length of the primary track to be measured is determined by the scanner: the track ends at the onset of the first clearly visible change in curvature of the electron. The reconstruction in TVGP is done as follows. The spectrum of photons radiated by a fast electron is integrated over the "soft photon" region, where "soft photons" means photons whose energies are small enough so that there is no visible, sharp change in curvature of the radiating electron track. The cut-off is taken such that an electron on the average gives up 39% of its energy in traversing one radiation length of material. This radiated energy loss is included in the energy loss calculated

* Present Nevis version.

by the range–energy subroutines in TVGP. Each electron track is measured with 20–30 points per view and reconstructed the r.m.s. deviations of the measured points from the fit calculated. The track is then cut back 10% in length (internally in TVGP) and reconstructed again. This is done up to ten times so that a table of lengths and r.m.s. is obtained. The iteration used for the final electron track parameters uses the longest length with an r.m.s. less than 1.2 times the minimum r.m.s. In other words, we pick the length of the electron track that gives the best fit to the model that the electron loses 39% of its energy in one radiation length.

With increasing momentum of the primary electron, it becomes more difficult to detect visually and/or by fitting methods small changes of curvature, which (mainly in the early part of the track) are due to a loss of a "hard photon". The method described above does not take into account such extreme cases. It is therefore interesting to compare results of the momentum measurements of the primary electron, which include only soft gammas, with the measurements including all converted primary high energetic gammas. This can be done in our calibration experiment, because we know the energy of the incoming electron. We are then able to establish criteria for the selection of the "correct" converted primary gammas. This is crucial in order to obtain good results: double counting of momenta can occur as well as gammas can be obscured and missed in very dense showers. A careful analysis of the measurements, in particular the azimuthal and dip angle of the pairs with respect to the direction of the primary electron, can help to solve most of the ambiguities related to double counting. The majority of secondary gammas will not be tangential to the primary electron.

2.2. Method (b)

Measurement of the total track length (TTL) of all electrons and positrons belonging to the electromagnetic shower [2]. This method is based on the relation between ionization loss and track length and requires that at least the hard component of the shower is completely contained inside the bubble chamber. The method reduces uncertainties due to the loss of hard bremsstrahlung, but has its limitation because of unmeasurably small or escaping low energy gammas. It was used successfully during the first neutrino experiment in the 1 m heavy liquid bubble chamber at the CERN PS [2]. Its accuracy is highly dependent upon the space in the chamber left for measurement.

In principle, this time-consuming TTL measurement of path lengths including all curvatures can be done by an automatic measuring machine. A fine-grid large area scan over the shower can establish the ratio of track to background surface. This method is only applicable when there are no hadron interactions in the region of the electromagnetic shower. Moreover, for large bubble chambers with bright-field illumination, this technique requires the subtraction of background originating from parasitic bubbles, Scotchlite imperfections, non-homogeneous illumination, etc. Also, a correction for the depth of the event in the chamber (change of optical magnification) must be done. All these factors together limit the precision and applicability of the automatic track length measurement. To our knowledge, automatic measurements of this kind have not yet been tried on a systematic basis.

2.3. Method (c)

Determination of the shower maximum in longitudinal direction (highest number of secondary tracks crossing a plane perpendicular to the direction of the primary electron). This method requires that an appreciable part of the shower beyond its maximum is visible on the photograph, and necessitates a comparison with a Monte Carlo calculation of the electron showers, which takes into account the influence of the magnetic field [3].

This method may provide an estimate for the momentum when the two other methods are not applicable. This may be the case if too little absorption length is available for method (a), or when the shower is not completely contained inside the chamber to get reliable results from method (b). The longitudinal shower maximum varies slowly with the momentum of the primary electron. The sensitivity of the method can be estimated from the well known calculations when no magnetic field is present, as described in ref. [4].

Some graphic results obtained by a Monte Carlo calculation [3], adapted to the magnetic field of the 15-ft chamber and the mixture used in our experiment, are enclosed in this report.

3. Selection of electrons for the measurement

We required that the following criteria were fulfilled during the scanning of the film:

a) Only one electron/picture should enter the bubble chamber.
b) No converted high energy gamma (with an estimated momentum > 1 GeV/c) is allowed, which may point to an origin other than the primary electron or its shower products.
c) No hadron interaction should be present, creating an electromagnetic shower, which cannot be separated easily from the primary electron and its shower products.
d) The estimated azimuthal angle of incidence of the primary electron (in the plane perpendicular to the magnetic field) should coincide with the angle of the beam within about $\pm 1°$.

Following the above scanning procedures, 33 pictures with one electron each were retained for further investigation.

4. Results of the measurements

Measurements were made on ~ 70 non-interacting hadron tracks to verify beam direction and momentum. The results of measurements show, that the mean value of the momenta is slightly higher than calculated from the setting of the beam transport elements, and that they have 0.7 GeV/c r.m.s. variations.

4.1. Results of method (a)

4.1.1. Measurement of the primary electron

The measurement of the momentum of the primary electron was done according to the standard procedures at Nevis and using the TVGP program. Fig. 1a shows the distribution of the measured momentum of the primary electrons. The histogram is fairly wide and the

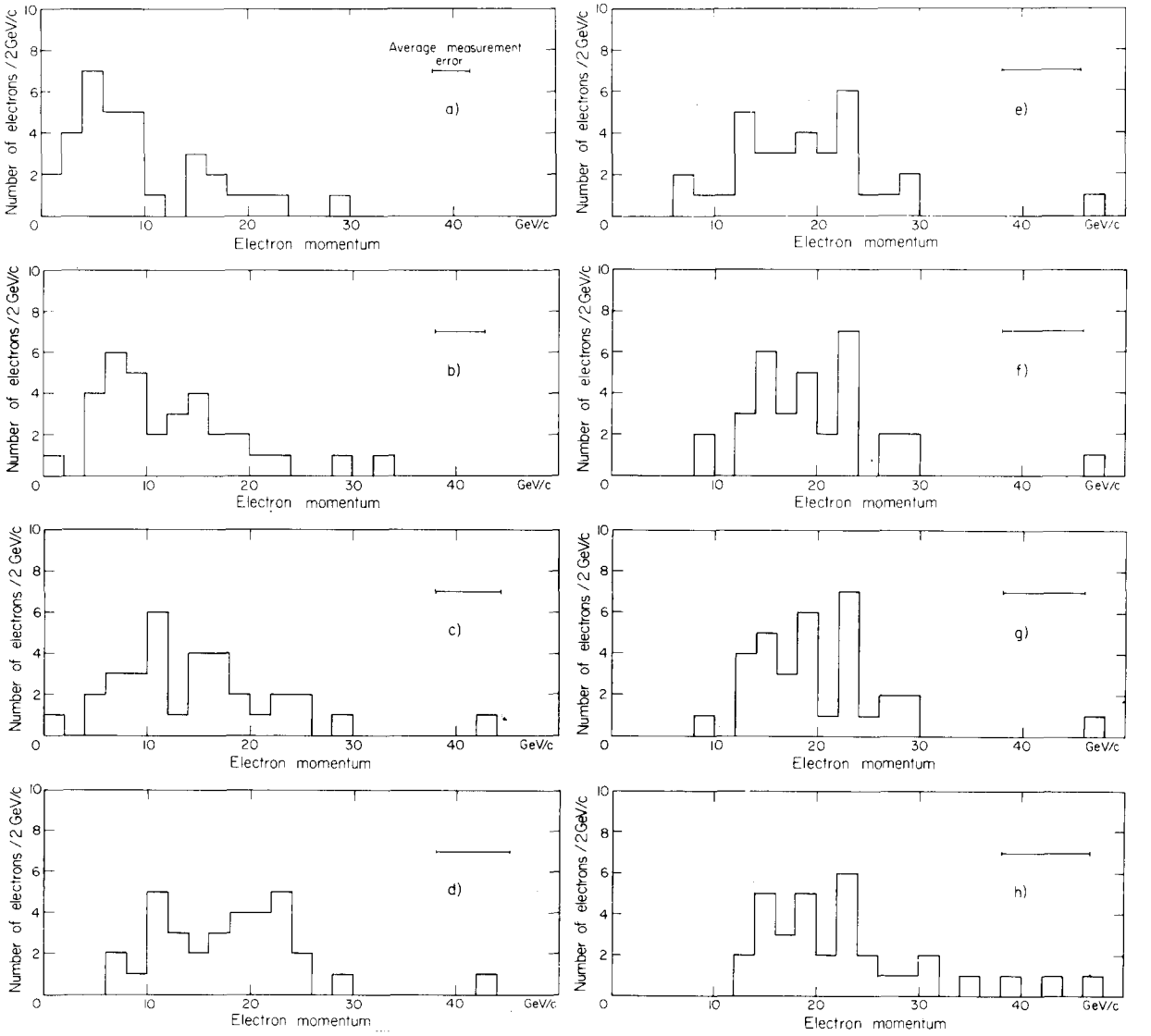

Fig. 1. (a) Measurement of the momentum from the curvature of the primary electron only. (b) Measurement of the momentum from the curvature of the primary electron, momenta of pairs emitted into an azimuthal angle of $\pm 0.3°$ added. (c) As (b) but azimuthal angle increased to $\pm 0.6°$. (d) As (b) but azimuthal angle increased to $\pm 0.9°$. (e) As (b) but azimuthal angle increased to $\pm 1.2°$. (f) As (b) but azimuthal angle increased to $\pm 1.5°$. (g) As (b) but azimuthal angle increased $\pm 1.8°$. (h) As (b) but all measured pairs added without azimuthal angle cut.

mean value is only about half the known beam momentum: P(primary electron) = (9.42 ± 6.88) GeV/c. This result is unsatisfactory and demonstrates the well known fact that energetic electrons lose in a statistical way large amounts of their energy by bremsstrahlung. To improve the result, one must add converted gammas pointing tangential to the early part of the track to the measured momentum of the primary electron.

4.1.2. Scanning for pairs

All those electron/positron pairs or Compton electrons were retained which were tangential to the early part of the primary electron (prior to a visible change in curvature) and which had an estimated energy of more than 0.6 GeV. They were sketched on a scan sheet together with the primary electron in order to facilitate the measurements and the final evaluation with the help of the computer output.

On the average, four pairs were traced together with each primary electron. The time needed for selecting and tracing the gammas was 20 min/event.

4.1.3. Measurement of the pair momentum and direction

The measurement of pairs follows the same pattern as used for primary electrons. The time needed is 90 min per complete event.

The line of flight of a gamma has to be determined from the direction of the two pair electrons at their vertex. In general the angle of each pair was taken as the mean of the angles of the electron and the positron track. Exceptions were made in the case of very asymmetric pairs: when the computed momentum of the two particles differed by more than a factor of 2 and simultaneously one of the partners had less than 1 GeV energy or the error on the angle of the low energy partner was $> 1.5°$, then the direction of the high energy partner was taken as gamma direction.

The average measurement errors of the azimuthal angle of all individual electrons and positrons, as given by the geometry output, was $\overline{\Delta\,\mathrm{PHI}}$ (electron, positron) = (1.12 ± 1.40)°. When we applied the above convention to find the gamma direction, this error was noticeably reduced to $\overline{\Delta\,\mathrm{PHI}}$ (gamma) = (0.75 ± 0.56)°.

The measured azimuthal angle of flight of gammas was used to keep only those pairs which can, with good confidence, be regarded as primary. The mean azimuthal angle of the electrons entering the bubble chamber liquid varies by ±0.55°, its mean angle at the cutoff point is determined by the measured length as accepted by the geometry program ($\bar{L}$ = 85 cm), the average magnetic field strength over this length (1.5 T) * and, if there were no large energy losses, would give a maximum deflection of 1.1°. The value of the latter can vary substantially. Therefore, we introduce only small additional uncertainties when we apply symmetrical cuts on the direction of flight of gammas in respect to the angle of electrons at their entrance into the chamber liquid.

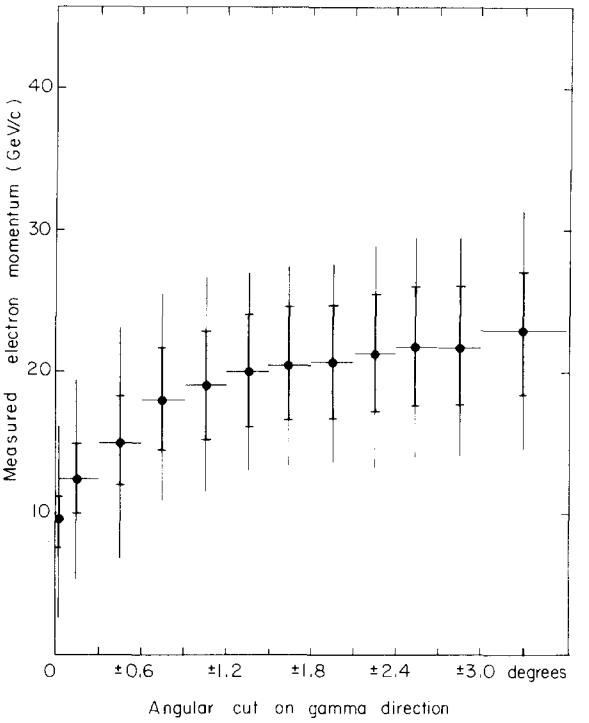

Fig. 2. Summry of figs. 1a–h: measurement of the momentum from curvature of the primary electron, momenta of pairs added and plotted as function of the angular cut on pairs; *thin bars*: mean value of 33 electrons and its standard deviaton; *thick bars*: average error from geometry output, errors from all tracks are added arithemetically.

Results, disregarding all gammas, and with various cuts and no cuts at all on scanned and measured gammas, are shown in fig. 1. The mean values of these historgrams are shown in fig. 2, the larger error bars indicate the standard deviation from the mean value of the sample, the smaller bars the measurement errors as given by the geometry output. From this figure we can estimate an optimum cut angle of ±1.2°. With this cut the mean value for the measured momentum is closest to the known beam momentum of 19 GeV/c.

The application of this method is simple, and gamma selection can be done reliably by scanners without special supervision by physicists.

4.1.4. Further tests of the validity of our gamma selection

In what follows, we try to check on the validity of the azimuthal angular cuts on gammas, their conversion points in electron positron pairs, their energy distri-

* The magnetic field at the entrance of the particles into the chamber in the nose cone is almost zero, and it reaches 3 T after about one radiation length.

bution as function of their distance from the entrance piont of the primary electron into the chamber, and finally to compare the experimental results with some theoretical estimates. In the following figures we averaged over all 33 events and normalized the results to one event. We measure the penetration depth of the primary electron and of the gammas in units of radiation length ($X_0 = 40$ cm for our mixture). The entrance point of the electron beam into the bubble chamber liquid is at $x = -265$ cm (counted from the centre of the bubble chamber).

In fig. 3, we plot the number of pair vertices in beam direction (x-direction) per radiation length. The outer envelope of the histogram contains all pairs as selected during the scan, the inner heavy curve shows the pairs retained after the $\pm 1.2°$ cut. As expected, a relatively large number of pairs downstream of the shower is rejected by this cut.

A plot of the momenta of gammas as function of their conversion point gives a more direct access to a comparison with theoretical estimates. In fig. 4 this distribution is given again with subdivision for various angular cuts. Here it is even more apparent that the rejection of gammas at large angles affects the final momentum determination insignificantly. Furthermore, ~ 80% of the total gamma energy is already converted into pairs during the first four radiation lengths.

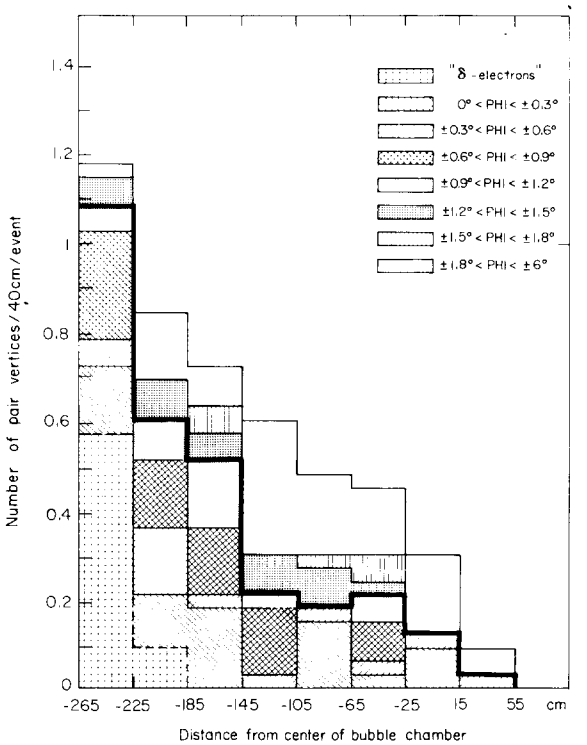

Fig. 3. Number of pair vertices/radiation length (40 cm intervals) in beam direction.

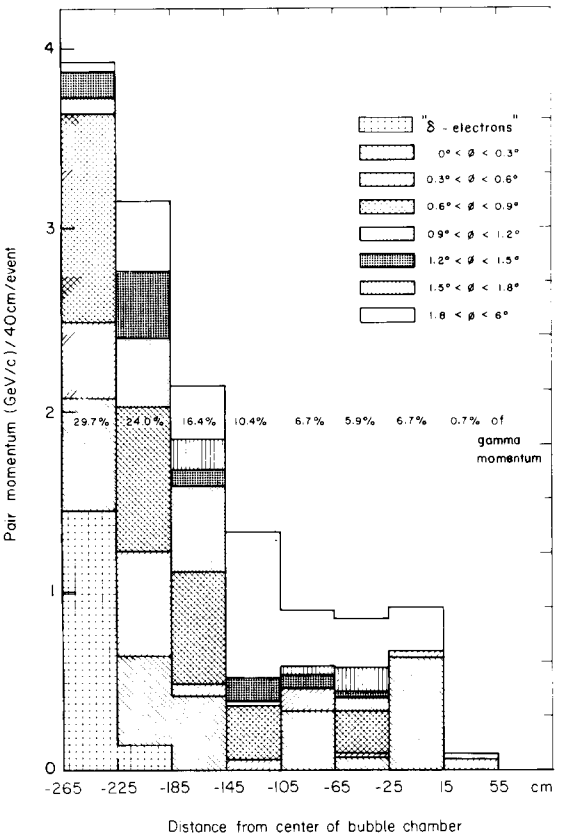

Fig. 4. Energy of gammas, converted into pairs/radiation length (40 cm intervals) in beam direction. The energy is grouped for various angular intervals. The percentage of the total energy which is converted per radiation length is given.

Figs. 5a and 5b show the number and moments of gammas in various azimuthal angle intervals, split into those going into the "correct" direction, i.e. following the curvature of the primary electron, and those going into the "wrong" direction. More than 70% of the energy of gammas is captured in the $\pm 1.2°$ interval.

Fig. 6 gives the gamma momenta integrated over angular intervals, and fig. 7 integrated over penetration depth, with angular cuts as parameter.

Now a crude comparison of these results with theoretical estimates can be done. We fold the probabilities of radiated energy, originating from the primary electron, with its absorption, and plot the result as function of traversed matter (fig. 8). In this plot, we give also the breakdown of the results obtained by considering only differential radiation losses, which occur in the first, the first two, etc. radiation lengths of the liquid. To estimate from which part of the primary electron track our gammas originated, and how much of and where this gamma energy is absorbed, we replot the curve for the energy of gammas converted as a function of position

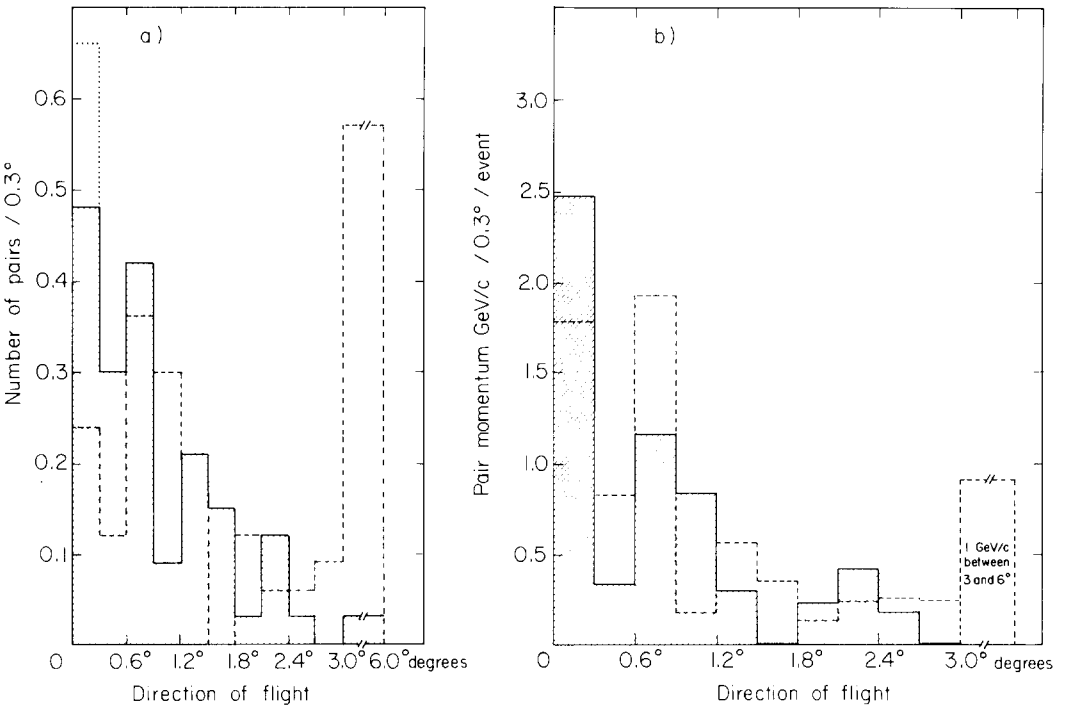

Fig. 5. (a, b) Number and momentum of pairs found in various azimuthal intervals, separated into pairs with direction following the curvature of the primary electron (tangential, dotted line), and those going into "wrong" direction (positive angle, solid line).

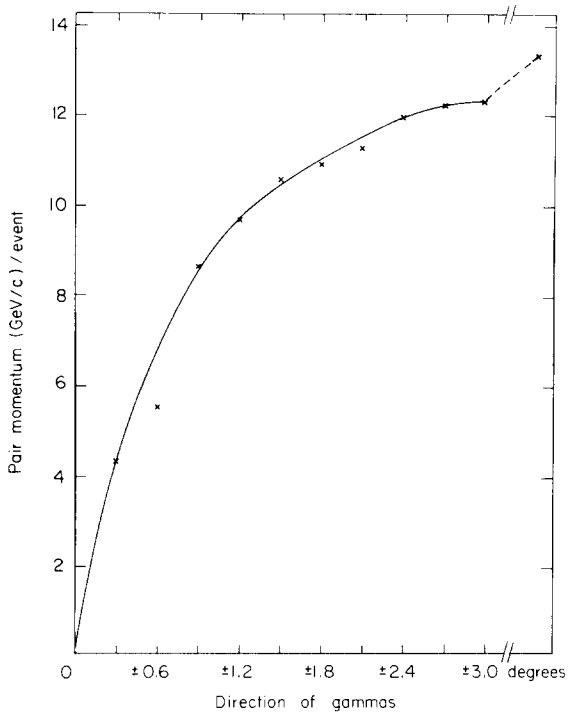

Fig. 6. Momentum of converted gammas, integrated over the azimuthal angle.

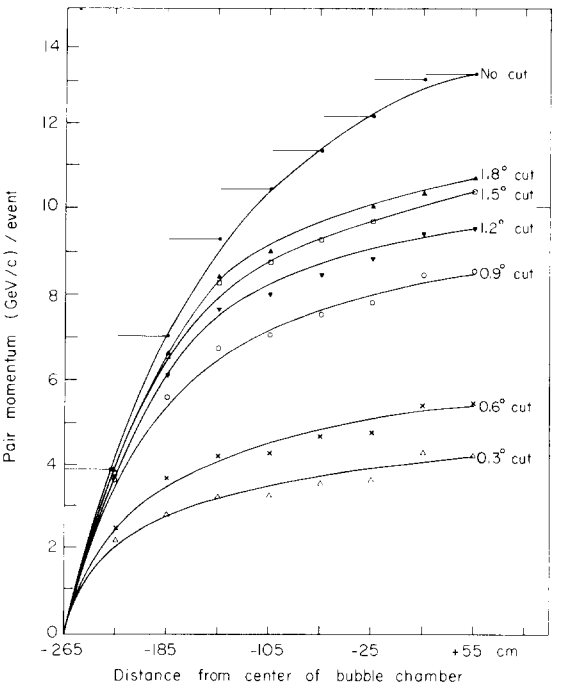

Fig. 7. Momentum of converted gammas, integrated over penetration depth, with various azimuthal angle cuts as parameter.

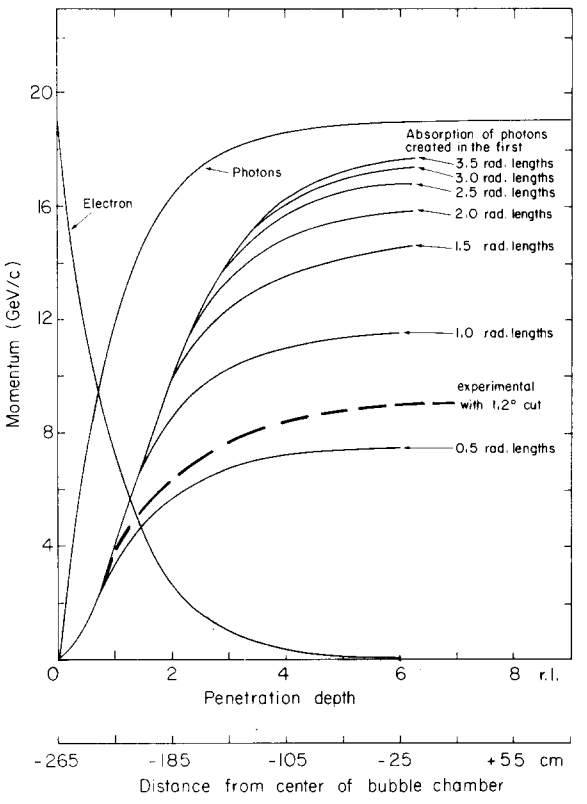

Fig. 8. Calculated energy of the primary electron as function of penetration depth, assuming only radiation losses. The total energy of the emitted photons is the mirror symmetric curve. The asorption of these photons as function of traversed material is given for photons created in the first 0.5, 1.0, 1.5, 2.0, 2.5, 3.0 and 3.5 radiation lengths, considering only absorption by pair creation. The dashed curve is the experimental result with all gammas within a $\pm 1.2°$ azimuthal angle.

along the electron track from fig. 7 (the fourth curve from the top for gammas within $\pm 1.2°$) as dashed line in fig. 8. The shape of the measured curve agrees well with those of the theoretical curves, and interpolating between the curves labelled 0.5 and 1.0 radiation length, we estimate that the gammas we select are radiated within the first 0.7 radiation length of the electron track. Looking at the curve labelled "electron" in fig. 8, we see that on the average the electron still has 9.5 GeV at 0.7 radiation length. This is consistent with the result [sect. 4.1 (a)] that the measurement of the momentum of the primary electron only gives 9.42 ± 6.88 GeV, and that the remaining 9.5 GeV is radiated into gammas, as seen from the experimental points plotted in fig. 8.

4.2. Results of method (b)

4.2.1. Measurement procedure at Nevis and error estimates

The measurement of the total track length (TTL) was done in low magnification (beam plane chamber/film $\sim 55/1$, film/scan table $\sim 1/13$) and in one view only. All four events were first traced on the scanning table on paper. These event sheets could then be measured at daylight. The track lengths were measured with a calibrated curve meter, each individual length was recorded and the track on the sheet was marked.

The measurements with the curve meter were reproducible on almost straight tracks; however, the measured length came out too small when the tracks terminated in tight spirals of less than 1 cm diameter. Therefore, we disregarded during the measurements such small spirals at the end of the track and also gammas of this size, which correspond to momenta 15 MeV/c. The overall reproducibility with our device is about $\pm 10\%$. Tracing and measuring of an event required between 2.5 and 3 h.

4.2.2. Interpretation of the measurements and conclusions

In order to translate the track lengths found on the scanning table into energies, we have to take into account the magnification scan table to bubble chamber (1 : 3.5), the dip angle of electrons out of the beam plane (projection factor ~ 1.1), and the collisions loss of electrons per unit path length. For the latter we chose somewhat arbitrarily for an average electron energy of 50 MeV the value of 1.77 MeV g^{-1} cm^2, because it is close to the track momenta that we disregarded during the measurement of spirals and delta-electrons. We obtain then for the electron momentum the values given in column 1 of table 1. These values are considerably smaller than the measured momentum from method (a) (column 6) and the known beam momentum. To account for the missing energy, we tentatively add the following amounts:

(a) At the end of each spiral ~ 3 cm track length (on the scan table) because we do not measure the length correctly due to the insufficiency of our curve meter. The result for the given number of electrons (column 2) is shown in column 3.

(b) Each measured pair may have produced either one ~ 40 MeV gamma or several less energetic gammas with a total energy of 40 MeV. We miss all gammas with energies smaller than about 40 MeV for two reasons:

(1) the cross section for pair production is down by a factor of ~ 4 in respect to the one at 1 GeV, and therefore most of these gammas escape, and

(2) we are unable to measure small pairs on the scan table in low magnification, which have a radius $\lesssim 0.5$ cm (for symmetric pairs this corresponds to 30 MeV). With the above assumption we

Table 1
Summary of results from method (b)

Momentum from measured track lengths (GeV/c)	Number of measured tracks	Corrections (GeV/c) for		Total momentum from TTL with corrections (GeV/c)	Total momentum from method (a) with $\pm 1.2°$ cut (GeV/c)
		losses by roller meter at end of tracks	lost low energy gammas		
Column 1	Column 2	Column 3	Column 4	Column 5	Column 6
10.73	155	2.11	6.26	19.04	23.14 ± 4.94
10.98	162	2.21	6.48	19.67	18.89 ± 0.67
9.38	160	2.18	6.40	17.90	18.16 ± 5.79
12.32	149	2.03	5.96	20.31	20.17 ± 5.34
10.83 ± 1.23	156 ± 6	2.13 ± 0.08	6.26 ± 0.23	19.23 ± 1.03	20.09 ± 2.20 4.18 ± 2.37

obtain the values of column 4 in table 1.

Assumption (a) accounts for some 25%, and assumption (2) for 75% of the momentum difference between column 1 and the nominal beam momentum.

4.2.3. Conclusions from method (b)

Method (b) may be made to work, but needs technical improvements and confirmation of various assumptions. The method is only applicable in cases when the total shower (or at least all energetic gammas) is contained inside the bubble chamber liquid. The depth of the shower (distance from the optics) must be known to determine the demagnification factor. A better estimate for escaping or unmeasurably small pairs must be available to apply corrections for missing energy. The method is very labor expensive, and any automatic measurements of TTL (e.g. on an HPD or ERASME) need a considerable programming effort.

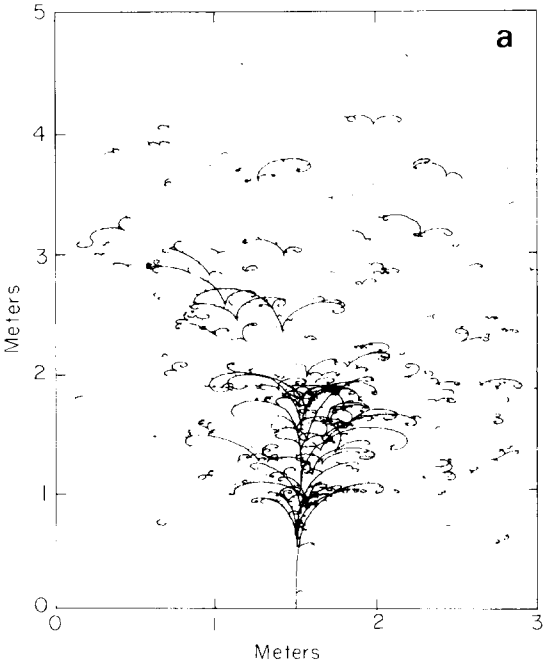

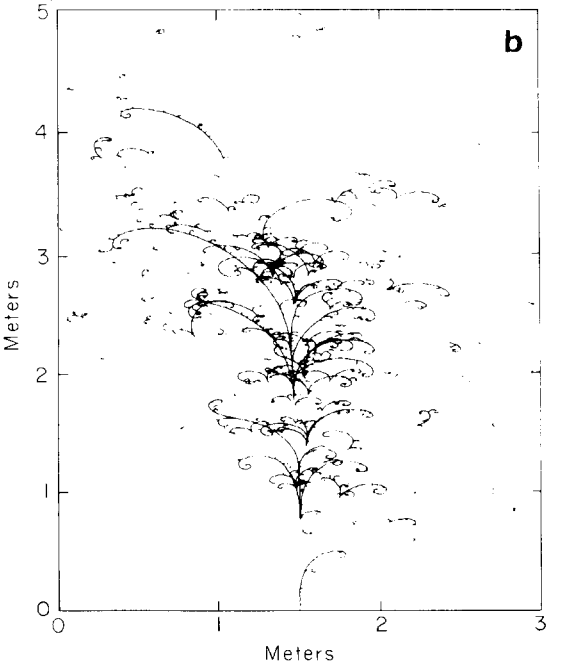

Fig. 9. (a, b) Monte Carlo produced electron showers in the heavy neon/hydrogen mixture used in the present experiment. Initial energy of the electron 19 GeV. Magnetic field 3 T.

4.3. Method (c)

4.3.1. Proposed measurement procedure

The direction of the primary electron has to be determined on the scan table. Then, equidistant planes perpendicular to this initial direction can be defined, separated for example by 0.15 radiation lengths. The distance of the event plane from the optics must be taken into account individually.

The procedure to determine the shower maximum in longitudinal direction would be to count the number of electron and positron tracks crossing the lines mentioned above.

We measured for the TTL method about 150 electron tracks per event with an estimated energy larger than 15 MeV, a number which should be sufficient for the present method to obtain the shower maximum. In order to evaluate the total shower over a distance of 10 radiation lengths (total length of the 15-ft bubble chamber's fiducial volume used for neutrino experiments), about 70 slices, each about 6 cm in real space, would be needed.

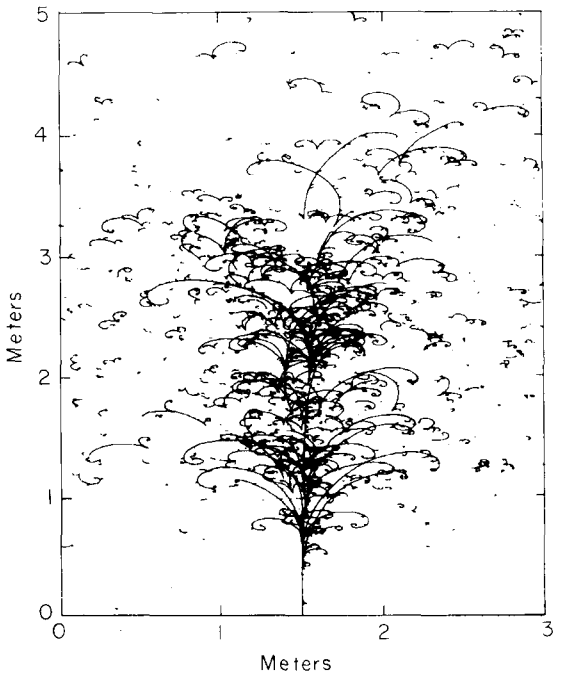

Fig. 10. Monte Carlo produced electron shower in heavy neon/hydrogen mixture used in the present experiment. Initial energy of the electron 50 GeV. Magnetic field 3 T.

4.3.2. Monte Carlo calculations

Grant [3] ran his Monte Carlo program for electron shower development for two electron momenta (19 GeV/c and 50 GeV/c) using the chamber conditions of the calibration run. Figs. 9a and 9b display the graphic results for 19 GeV/c, and fig. 10 for a 50 GeV/c electron.

Fig. 9 demonstrates that for our experiment most of the hard component of the electromagnetic shower is materialized and contained inside the bubble chamber.

It is possible to adjust the computer program such that it gives the number of electrons (positrons) traversing predetermined planes, as described in sect. 4.3.1, and hence to find the longitudinal shower maximum.

5. Comparison of the three methods

Quantitative results from measurements are obtained until now only from the first two methods. Clear preference has to be given to method (a), both from the view of applicability for actual neutrino events occurring everywhere in the chamber, and from the view of precision and time requirement. Method (b) could become interesting for fully automatic measuring machines.

This experiment would not have been possible without the continuous support of the Neutrino Department at Fermilab, the dedicated efforts of the operation group of the 15-ft bubble chamber, and the designers and operators of the beam, in particular, L. Stutte and G. Kuozomi. The painstaking and patient work of the scanners at Nevis Laboratories is gratefully acknowledged. We are very grateful to A. Grant from CERN, who produced the shower pictures with his Monte Carlo program. We also thank the National Science Foundation for its support of this research.

References

[1] E. Schmidt, Ph.D. Thesis, Columbia University, Nevis Report 224 (1978) p. 65.
[2] H. Burmeister, G. von Dardel and K. Schultze, Proc. Sienna Int. Conf. on Elementary particles (1963) vol. 1, p. 552.
[3] A. Grant, Nucl. Instr. and Meth. 131 (1975) 167.
[4] B. Rossi, High energy particles (Prentice Hall, 1952); W. Heitler, The quantum theory of radiation, 3rd ed. (Clarendon Press, Oxford, 1954).